JAERI-Research
98-057

CALCULATION OF NEUTRON FLUX CHARACTERISTICS OF DALAT REACTOR USING MCNP4A CODE

October 1998

Tran Van HUNG, Yukio SAKAMOTO and Hideshi YASUDA

日本原子力研究所
Japan Atomic Energy Research Institute

本レポートは，日本原子力研究所が不定期に公刊している研究報告書です。
入手の問合わせは，日本原子力研究所研究情報部研究情報課（〒319-1195　茨城県那珂郡東海村）あて，お申し越しください。なお，このほかに財団法人原子力弘済会資料センター〒319-1195　茨城県那珂郡東海村日本原子力研究所内）で複写による実費領布をおこなっております。

This report is issued irregularly.
Inquiries about availability of the reports should be addressed to Research Information Division, Department of Intellectual Resources, Japan Atomic Energy Research Institute, Tokai-mura, Naka-gun, Ibaraki-ken 319-1195, Japan.

編集兼発行　日本原子力研究所

Calculation of Neutron Flux Characteristics of Dalat Reactor Using MCNP4A Code

Tran Van HUNG*, Yukio SAKAMOTO and Hideshi YASUDA

Center for Neutron Science
Tokai Research Establishment
Japan Atomic Energy Research Institute
Tokai-mura, Naka-gun, Ibaraki-ken

(Received September 9, 1998)

The neutron flux characteristics of the Dalat reactor such as energy spectra, absolute neutron flux and neutron flux distribution along an irradiation channel were calculated by using MCNP4P code. All computations were done on a personal computer with the running time about 2 days for every case. The calculation configuration is similar to real one of reactor at the nominal power 500 kW. The calculated results of neutron flux and a spectrum fitting parameter, α , are in good agreement with experimental ones within 5%.

By using the calculated energy spectra, the cadmium ratios (R_{cd}) and effective cross-section of ^{197}Au in the irradiation channels were calculated. In this calculation, were used the multi-group cross-sections of ^{197}Au from Japanese Evaluated Nuclear Data Library (JENDL) and International Reactor Dosimetry File 82 (IRDF82). The comparison of the calculated results shows that : (1) the difference of R_{cd} values between the experiment and calculation using cross-section of $^{197}Au(n,\gamma)^{198}Au$ reaction is 1 to 6% for IRDF82 and 4 to 8% for JENDL, and (2) the effective cross-sections of $^{197}Au(n,\gamma)^{198}Au$ reaction from IRDF82 and JENDL dosimetry files are completely in good agreement with each other.

Keyword : Calculation, Experiment, Configuration, Distribution, Neutron Flux, Dalat Reactor, MCNP4A Code, Cadmium Ratio, Neutron Spectrum, Personal Computer

---

*STA Scientist Exchange Program (Dalat Nuclear Research Institute, VIETNAM)

MCNP4Aコードによるダラット炉の中性子束特性計算

日本原子力研究所東海研究所中性子科学研究センター
Tran Van HUNG*・坂本 幸夫・安田 秀志

（1998年9月9日受理）

Dalat炉の中性子束特性であるエネルギースペクトル、中性子束絶対値及び照射孔に沿った分布をMCNP4Aコードで計算した。すべての計算はパーソナルコンピュータで実施した。各ケースの計算時間は約2日であった。計算体系は500Wで運転される炉心を正確にモデル化した。中性子束及びスペクトルフィッティング因子 α は5%以内で実験値と一致した。計算で得たエネルギースペクトルを用いてカドミウム比及び^{197}Auの実効断面積を計算した。この計算ではJENDL及びIRDF82の核データを用いた。計算結果の比較から、(1)カドミウム比は計算値/実験値がIRDF82の場合に1～6%、JENDLの場合に4～8%であり、(2)^{197}Au (n, γ) ^{198}Au実効断面積はJENDLまたはIRDF82を用いても殆ど同一の値を与えた。

東海研究所：〒319-1195 茨城県那珂郡東海村白方白根2-4
* 科学技術庁原子力研究交流制度研究員（ベトナム ダラット原子力研究所）

Contents

目　　次

This is a blank page.

1. Introduction

The Dalat reactor is a pool-type research reactor, which uses water as the coolant and the moderator. It was rebuilt from 250 kW TRIGA MARK II reactor in 1984. By the reconstruction, the nominal power was increased to 500 kW. The present working configuration of the reactor core includes 100 fuel elements, 2 safety rods, 4 shim rods, 1 regulating rod, 2 dry irradiation channels, and 2 wet irradiation channels. The central channel is encircled by a beryllium layer, which traps thermal neutron. Therefore, it is called "neutron trap". The outside of active core is a graphite reflector. All of reactor core is submerged in a water tank of 6.26 m height and 1.98 m diameter.

The characteristics of the neutron flux in irradiation channels have been determined by experiments. The experimental method and results used in this paper were reported in a previous work [1]. However, the reliable calculations of these characteristics are necessary to examine the experimental results, specially, for absolute values. In the experiments, the determination of the absolute values of neutron flux in the neutron trap and 1-4 channel have a hindrance, due to the fact that the irradiation sample is placed and removed manually, without pneumatic system, so that the accurate control of irradiation time is difficult.

In this report, the neutron flux characteristics such as energy spectra, absolute neutron flux and distribution of neutron flux in irradiation channels are calculated by using a Monte Carlo code.

2. Calculation

2.1 Calculation Code and Computer

The MCNP4A code is chosen for the calculation in this problem. The MCNP4A [2] is a useful nuclear physics computer code and used widely in the world. At present, this code can be run on a personal computer and is not limited to a super computer since a few years ago [3].

In the present work, the calculations were performed on the personal computer (MMX Pentium 200 MHz).

2.2 Dalat Reactor Description

The Dalat reactor is a pool type research reactor. Distilled water is used as moderator, coolant, reflector and biological protection. The cylindrical reactor is arranged symmetrically by several kinds of material elements. In the center of active region is a neutron trap of radius 3.2 cm. The fuel elements, beryllium and graphite blocks, control rods and irradiation channels are the active region of reactor and form a hexagonal prism lattice in the cylindrical reactor with radius 20.8 cm and height 60.0 cm. Outside of the active region is a graphite reflector with thickness of 32.6 cm. The working configuration of reactor core is shown in Fig. 1. The structure and dimension of fuel elements, control rods and others are as follows:

2.2.1 Fuel Elements

The structure and dimension of fuel elements are shown in Fig. 2. The fuel element is bundle type and composed of 3 concentric tubes: 2 circular inner tubes and a hexagonal outer tube. The fuel tubes are 0.7 mm thick and are wrapped with the 0.9 mm thick aluminum cladding. Outside of the aluminum cladding layer is coolant water. The fuel material is uranium with the enrichment of ^{235}U of 36% and has a density of 1.51 g/cm^3. The active length of a fuel element is 60 cm.

2.2.2 Control Rods

There are three types of control rods. They are shim, safety and regulating rods. The outer structure and dimension of control rods are same as those of fuel elements. In Fig.1, the 4 shim rods (marked by KC1, KC2, KC3, KC4) and 2 safety rods (marked by AZ1, AZ2) are arranged symmetrically in the active region. The regulating rod is made of stainless steel and located at (7,11) element (marked by AR). The shim and safety rods are made of boron carbide with density of 2.05 g/cm^3 wrapped with 1 mm thick aluminum.

2.2.3 Irradiation Channels

The Dalat reactor has two types of irradiation channels; wet and dry irradiation channels. The wet irradiation channel is a cylindrical water column of 1.4 cm radius and encircled by an aluminum tube. The dry irradiation channel includes two parts; a central air column of 1cm radius and a hexagonal surrounding water layer.

In Fig. 1, the address of an element is indicated by two numbers, one is the order from left to right and another is from top to bottom. So that, first irradiation channel is located at (1,4) element and called 1-4 channel. It is a wet irradiation channel. Similarly, 13-2 and 7-1 channels are located at (13,2) and (7,1) elements, respectively. They are dry irradiation channels. The neutron trap is also a wet channel, but it's structure is different from 1-4 channel. The neutron trap is located at the center of the active region. It is water column of 3.2 cm radius and is encircled by the beryllium layer.

2.2.4 Beryllium and Graphite Blocks

Beryllium and graphite blocks are simply solid material with density of 1.875 g/cm^3 and 1.68 g/cm^3, respectively.

2.3 MCNP Model Description

2.3.1 Calculation Model

The reactor core configuration was modeled following the real one realistically. However, for simplicity in model description, the structure of fuel element along the length was divided into three zones. The central zone; fuel contained zone, is described accurately and both end zones are described with the homogenous mixture of aluminum and water with an average density of 1.319 g/cm^3. The actual and model structures of the fuel elements are shown in Fig.2.

When reactor was operated at 500 kW without the irradiation sample, 4 shim rods were elevated up to 16 cm from the bottom of active region, therefore, this condition was taken into account. Two safety rods and the regulating rod are pulled up over the active region. Therefore, they are water columns in the calculation model.

The model structures of graphite and beryllium block and graphite reflector are completely the same as the actual ones.

The material data used in the calculation model are presented in Table 1.

2.3.2 Source and Tally

In the present problem, KCODE (criticality problem) and KSRC (initial spatial distribution of source points) cards are used for the source description. In this case, MCNP offers several options for the K_{eff} value estimate, including the combined average of the absorption, collision and track-length estimator.

For all calculations of neutron flux and spectra, the F4 tally was used. F4 is a track-length tally card for calculating average neutron flux over a cell. However, in some case, for comparison, the F5 tally was also used. It is a point detector tally for the calculation of neutron flux at a point in space. It can provide a good estimate of the neutron flux where would be almost impossible to get by either track-length (F4) or other tallies. The flux at a point cannot be estimated by a track-length tally (F4) or a surface flux tally (F2), because the probability of a track entering the volume or crossing the surface of a point is zero.

The experimental results are given in terms of flux, neutron/cm^2/s at 500 kW operation, on the other hand, MCNP tallies give fluence in unit, 1 neutron/cm^2, caused by one source neutron. For the comparison with experiment, the MCNP results can be properly normalized using the following conversion factor:

$$\left(\frac{1\ \text{joule/s}}{\text{W}}\right)\left(\frac{1\text{MeV}}{1.602\text{x}10^{-13}\ \text{joule}}\right)\left(\frac{1\text{fission}}{200\ \text{MeV}}\right) = 3.12\text{x}10^{10}\ (\text{fission/W·s}) \qquad (1)$$

For the Dalat reactor at nominal power of 500 kW, the scaling factor is

$$(0.5\ \text{MW})\left(\frac{1\text{neutron/cm}^2}{\text{source}}\right)\left(\frac{2.4\text{source}}{\text{fission}}\right)\left(\frac{10^6\ \text{W}}{1\ \text{MW}}\right)\left(\frac{3.12\text{x}10^{10}\ \text{fission}}{\text{W·s}}\right) = 3.744\text{x}10^{16}\text{n/cm}^2\text{·s} \qquad (2)$$

It means that the value of neutron flux (1 neutron/cm^2) in OUPUT of MCNP4A has to be multiplied by the scaling factor 3.744x10^{16} for the Dalat reactor at 500 kW operation.

In the calculation, the neutron energy range from 0 to 20 MeV was divided into 112 groups.

2.3.3 Cross-section Libraries

Nuclide cross-sections were taken from JENDL-3.2 [4]. In calculation, the S(α,β) thermal treatment was also used for H_2O, beryllium and graphite.

A plan view of the calculation configuration obtained from INPUT deck description is shown in Fig. 3. We can confirm that INPUT deck described faithfully the working configuration shown in Fig.1. An INPUT sample for calculation of energy spectrum, neutron flux and its distribution in neutron trap and 1-4 channel is shown in Appendix.

3 Calculation Results and Discussions

3.1 The Neutron Flux in Irradiation Channels

The calculated k_{eff} value was 1.0010 ± 0.0005. The calculation simulated a critical state. Therefore, this value is quite satisfactory. Absolute values of maximal thermal neutron flux at 1-4, 13-2, 7-1 channels and neutron trap are presented in Table 2. In this table, neutron flux is evaluated at experimentally maximal positions for neutron trap and 1-4 channel and at the sample irradiation positions for 7-1 and 13-2 channels.

In the experiment [1], the activation method was used for the determination of neutron flux characteristics in irradiation channel. This method is described in detail in paper [5]. Au-foils were used as the neutron flux monitors, because gold has excellent properties as a capture standard. The sample preparation is particularly easy, since the material is monoisotopic and the product nucleus has a simple decay scheme, especially, it's cross sections has been determined in detail and with high accuracy. For determination of neutron flux distribution along the vertical irradiation channel, the bare Au-foils were fixed at different positions along the length of an organic glass sheet and irradiated for about 5 minutes at the reactor power of 500 kW. The gamma-ray intensity of ^{198}Au was measured by a high purity Ge detector of 70 cm^3 coupled to a multi-channel spectrometer. The relative neutron flux at position (i) was determined by:

$$\frac{\phi_i}{\phi_{max}} = \frac{A_i}{A_{max}} \qquad (3)$$

where, A_i and A_{max} are gamma-ray intensities of ^{198}Au at *(i)* and maximal flux positions, ϕ_i and ϕ_{max} are neutron flux at position *(i)* and maximal flux, respectively. In the experiment, the maximal flux position was at 25 cm from the bottom of active region.

Absolute thermal neutron flux was determined by using the formula:

$$\phi_{th}(n.cm^{-2}.s^{-1}) = \frac{S\,A}{m\,\sigma_{act}\,\varepsilon\,\gamma\,N_0} / (1-e^{-\lambda t_{irr}})e^{-\lambda t_c}(1-e^{-\lambda t_m}) \qquad (4)$$

where m; weight of gold in foil (g), σ_{act}; activation cross section of ^{197}Au (barn), N_0 ; Avogadro number (6.023×10^{23}), A; mass number of gold, λ ; decay constant of ^{198}Au , t_{irr} ; irradiation time, t_c ; cooling time, t_m; measuring time, ε; efficiency of detector, γ ; emission rate of the gamma ray, S ; area of the gamma ray peak.

In formula (4), the error of the absolute value of the neutron flux in the experiment depends on many factors. Therefore, the accurate determination of absolute neutron flux is difficult, especially, in 1-4 channel and neutron trap due to the inaccurate irradiation time.

As shown in Table 2, the absolute thermal neutron flux in the irradiation channel is calculated with high level of accuracy. As the calculation check, the F4 and F5 tally cards were simultaneously used in some calculations. The results obtained from both tallies were similar. For example, when calculating the neutron flux at position of 22 cm from the bottom of active region in neutron trap, the calculated results are $(1.23\pm0.07)\times10^{-3}$ neutron/cm^2 and $(1.18\pm0.007)\times10^{-3}$ neutron/cm^2 by using F5 and F4 tallies, respectively. The relative uncertainty of calculated results using F5 tally is ten times larger.

The comparison of calculated and experimental values of the absolute neutron flux shows that both values are in good agreement with each other. The difference between calculated and experimental values are less than 5%. The relative error in the Table 2 is less than 1% for MCNP calculation and 5% for experimental data.

The distributions of neutron flux along 1-4 channel and neutron trap are shown in Fig.4 and Fig.5, respectively. In these figures, neutron flux distributions are normalized at 30 cm position. The neutron flux distributions in irradiation channels also correspond to experimental ones by their appearance and positions of maximal values. The maximal flux position in the experimental data locates at 25 cm from the bottom of the active region. In the MCNP calculation results, it locates at about 24 cm. In the Fig. 4 and Fig. 5, the appearances of the distributions in 1-4 channel and neutron trap are quite similar. At the height about 15 cm from the bottom of active region, the calculated and experimental neutron fluxes are lower than fitting curve and the neutron flux distribution is not a symmetric cosine function. It can be explained by the effect of control rods. During the reactor operation, the control rods were pulled up to 16 cm from the bottom of active region.

3.2 Energy Spectra

The important characteristics of irradiation positions are thermal, epi-thermal neutron fluxes and α-factor. We know that, in many cases, the epi-thermal neutron flux distribution is not proportional to 1/E, but rather $1/E^{1+\alpha}$, where α is a small positive or negative constant between −0.1 and 0.1. The neutron energy spectrum was calculated at different positions along the vertical irradiation channels. In Fig. 6 and Fig. 7 are shown the calculated energy spectra at position 22cm in the neutron trap and 1-4 channel.

Neutron spectrum at an irradiation position can be expressed as a sum of a thermal equilibrium spectrum; $\varphi_{th}(E)$ (Maxwellian distribution, neutron energy from 0 to 0.5 eV) and epi-thermal spectrum in the slowing down region; $\varphi_{epi}(E)$ (neutron energy from 0.5 eV to maximal). In the paper [5], the neutron spectra were fit on a semi-empirical function:

$$\varphi_{th}(E) = I_{th} \cdot (E/E_T^2).e^{-E/E_T} \qquad (5)$$

and

$$\varphi_{epi}(E) = I_{epi}.(E/1eV)^{-\alpha}.1/E \qquad (6)$$

where, $I_{th}(E)$ and $I_{epi}(E)$ are scaling constants for the thermal and epi-thermal portion, E_T is a characteristic energy of the Maxwellian portion of the spectrum.

In the present work, $I_{th}(E)$, $I_{epi}(E)$, E_T and α are determined by fitting the calculated neutron spectra on Eqs. (5) and (6). The fitting results are shown in Tables 3 and 4.

The relative error of the calculated spectrum intensity in each energy group was less than 5%, especially, in thermal neutron region was less than 2%. Consequently, the fitting parameters I_{th} and E_T are obtained with relative error of about 2%. In the epi-thermal region, fitting parameter I_{epi} was obtained with the similar relative error of 2%, but α factor with the relative error about 10%. From the experimental data, α factor was also obtained with a less accuracy. Perhaps, this is because α is small power constant standing for a wide energy region, in addition, the proportion of $1/E^{1+\alpha}$ is an approximation in the formula (6). The method for the determination of experimental α-factor is described in detail in Ref. [6].

The E_T-fitting values in these tables demonstrate that neutron thermalization in neutron trap is better than in 1-4 channel. This is because the neutron trap is well moderated with water and beryllium layers.

The comparison of the α-factors in Table 5 shows that the calculated values agree well with experimental ones. The difference between both data is 6%.

In order to examine the calculated spectra, the cadmium ratios (R_{Cd}) of ^{197}Au in the irradiation channels were also calculated. R_{Cd} of an isotope is defined as the ratio of the measured activities of the sample with and without a cadmium cover. It can be easily evaluated from the experiment by activating monitor foils. Au-foils were used as monitors in this experiment. The experimental cadmium ratio at the irradiation position is determined by:

$$R_{Cd} = \frac{A_{bar}}{A_{Cd}} \qquad (7)$$

where, A_{Cd} and A_{bar} are gamma-ray intensities of ^{198}Au produced in the irradiated foils with and without a cadmium filter, respectively. In the experiment, cadmium filter thickness was 0.8 mm.

In the calculation, R_{cd} of gold can be approximated as follows:

$$R_{Cd} = \frac{\int_0^{\infty} \sigma(E).\phi(E)\,dE}{\int_{E_{Cd}}^{\infty} \sigma(E).\phi(E)dE} \qquad (8)$$

where, $\sigma(E)$ and $\phi(E)$ are (n,γ) cross-section of gold and neutron spectrum, E_{Cd} is the cadmium cut-off energy. In many references, E_{Cd} are chosen to about 0.5 eV. However, the chosen cut-off energy E_{Cd} depends on the shape and thickness of the Cd filter. For that reason, in this work the cadmium ratio is calculated by:

$$R_{Cd} = \frac{\int_0^{\infty} \sigma(E).\phi(E)\,dE}{\int_0^{\infty} \sigma(E).\eta(E).\phi(E)dE} \qquad (9)$$

and $$\eta(E) = EXP\{-N.\sigma_t(E).d\} \qquad (10)$$

where, $\eta(E)$ is the transmission factor of neutron beam of energy E through Cd filter of thickness d (cm) with N atoms per cm^3, $\sigma_t(E)$ is total cross-section of cadmium.

The calculated result of the neutron transmission factor $\eta(E)$ for cadmium with 0.8mm thickness is shown in Fig.8. In this figure, we can see that cadmium filter completely absorbs thermal neutrons, transmitting the neutrons of above 1eV energy. However, in resonance region the neutrons are not completely transmitted through the cadmium filter, especially, at the resonance peaks of cadmium. For comparison, the cadmium ratios were also calculated by using formula (8) with the chosen cut-off energy E_{Cd} = 0.5 eV. However, the difference of R_{Cd} between formula (8) and (9) were less than 3%.

The calculated R_{Cd} ratios are presented in Table 6. The cross-sections of gold were taken from the International Reactor Dosimetry File 82 (IRDF-82) [7,8] and JENDL Dosimetry File [9]. For simplicity, the JENDL Dosimetry File and IRDF-82 are denoted as JENDL and

IRDF in the following descriptions. The multi-group cross-sections of $^{197}Au(n,\gamma)^{198}Au$ reaction in IRDF and JENDL are shown in Fig.9. In the energy region from 0 to 100 eV, the cross-section values of two libraries are very close each other. But in the energy region above 100 eV there is a little difference between them, especially, in the E_n >3.5 MeV region. However, the difference of cross-section of ^{197}Au in energy region above 3.5 MeV will not affect the calculated results of cadmium ratios because of the small cross-section and the low flux.

The uncertainty of the calculated R_{Cd} ratio should depend on the uncertainties of the calculated neutron intensity and cross-section of gold in each energy group. However, the errors in Table 6 are 5 to 8% which takes account only of the uncertainty of calculated neutron intensity. The comparisons of R_{Cd} ratios showed that all the calculated results are higher than the experimental ones. In the experiment, the R_{Cd} ratio was determined by irradiating two Au-foils of with and without cadmium covers and adjacent each other at a time. The R_{Cd} ratio was not paid attention to the thermal neutron flux disturbance. Therefore, the activity of Au-foil without cadmium cover is lower. That conduced the cadmium ratio obtained from formula (7) is lower than actual value. Thus, the experimental values of the cadmium ratios must be corrected for the disturbance of neutron field caused by cadmium filter.

The difference of R_{Cd} values between the experiment and calculation using cross-section of $^{197}Au(n,\gamma)^{198}Au$ reaction is 1 to 6% for IRDF and 4 to 8% for JENDL, and the difference between two calculated values is only 2%. This difference is mainly caused by the difference of cross-sections in the resonance energy region.

Through the comparison of cadmium ratios between the calculations and experiments, it should be noted that the energy spectra calculated with MCNP are accurate from this view point.

To evaluate the practical difference of multi-group cross-sections between two libraries, the effective cross-sections of $^{197}Au(n,\gamma)^{198}Au$ reaction in the neutron trap and 1-4 channel were calculated by using the calculated neutron spectra and the multi-group cross-sections of $^{197}Au(n,\gamma)^{198}Au$ reaction from IRDF and JENDL following the definition:

$$\sigma_{eff} = \frac{\int_0^{\infty} \sigma(E).\,\phi(E)\,dE}{\int_0^{\infty} \phi(E)dE} \qquad (11)$$

The calculated effective cross-sections are presented in Table 7. The results show that the effective cross-sections of $^{197}Au(n,\gamma)^{198}Au$ reaction in two these libraries agreed well each other within the difference of 1%.

4. Conclusion

The use of MCNP4A code on a personal computer Pentium 200 MHz, 32 Mbite memory with MMX is very successful for the calculation of the neutron flux and energy

spectrum of Dalat reactor. The obtained results are accurate with the relative error of <1% for neutron flux and 5% for energy spectrum by the running time of the computer from 2 to 3 days. All calculated results are in good agreement with experimental values.

The simplification of the calculation model for the fuel element did not lose the faithfulness of MCNP simulation performance. The value obtained from these MCNP calculations can be used to estimate and examine the experimental results.

From the calculation of the cadmium ratios and the effective cross-sections of $^{197}Au(n,\gamma)^{198}Au$ reaction at the irradiation positions, it was revealed that the uses of the multi-group cross-sections from IRDF82 and JENDL Dosimetry File are completely equivalent.

Acknowledgments

The authors would like to thank Dr. Takehiko MUKAIYAMA, director of Center for Neutron Science, JAERI, for his interest and support in all the work. The authors also would like to thank Dr. Makoto TESHIGAWARA, Mr. Tadashi NAGAO, Mr. Shin-ichiro MEIGO, Mr. Yoshihiro NAKANE, Mr. Masanobu IBARAKI for their discussions and effective assistance in computations.

References

(1) HUNG. T. V: " Determination of Some Characteristics of Neutron Flux of Dalat Reactor for Neutron Activation Analysis and Radioisotope Production", Proceedings of the first National Conference on Nuclear Physics and Techniques, Hanoi, 15-16 May, p.85 (1996) (In Vietnamese).
(2) BRIESMEISTER R. F: " MCNP –A General Monte Carlo N-Particle Transport Code, Version 4A," LA-12625, Ed., Los Alamos National Laboratory Report (1993).
(3) HENDRICKS J. S., BROCKHOFF R. C.: Nucl. Sci. Eng., 116, p. 269-277 (1994).
(4) SHIBATA K., et al.: " Japanese Evaluated Nuclear Data Library, Version 3 –JENDL-3-," JAERI 1319, Japan Atomic Energy Research Institute (1990).
(5) CARPENTER J. M., et al.: Nucl. Instrum. Methods Phys Res., A234, 542 (1985).
(6) De COTRTE F., et al.: J. Radioanal. Chem., 62, 209 (1981).
(7) GRYNTAKIS E., et al.: Thermal Neutron Cross-sections and Infinite Dilution Resonance Integrals, Technical Reports Series No. 273, IAEA, VIENNA, p.199-256 (1987).
(8) CULLEN D. E., et al.: Nucl. Sci. Eng.,Vol. 83(4), p.497-503 (1993).
(9) NAKAZAWA M., et al.: JENDL Dosimetry File, JAERI 1325, March (1992).

Table 1. Composition of materials used in the MCNP model

Material Unit	Materials	Symbol	Density (g/cm^3)	Weight Fraction
Fuel element (Central part)	- Uranium	M6	1.51	
	-^{235}U			0.36
	-^{238}U			0.64
	- Aluminum	M4	2.7	
	-Al-			1.0
Fuel element (End parts)	-H_2O+Al	M8	1.319	
	- Al			0.3846
	- H			0.06831
	- O			0.5469
Graphite block	- Graphite	M5	1.68	
	-C			0.995
	-Fe			0.0034
	-S			0.0016
Beryllium block	- Beryllium	M2	1.875	
	-Be			1.0
Coolant	- Water	M1	1.0	
	-O			0.889
	-H			0.111
Dry channel	- Air	M7	0.0012	
	-N			0.7818
	-O			0.2098
	-Ar			0.0085
	- Aluminum	M4	2.7	
	-Al			1.0
Control rod	-Boron Carbide			
	-^{10}B	M3	2.05	0.6870
	-^{11}B			0.0840
	- C			0.2290
	- Aluminum	M4	2.7	
	-Al			1.0
Wet channel	- Water	M1	1.0	
	- H			0.889
	- O			0.111

Table 2. The calculated and experimental absolute values of thermal neutron flux in the irradiation channels of Dalat reactor

Irradiation channel	Calculated neutron flux ($n/cm^2/s$)	Experimental neutron flux ($n/cm^2/s$)	Cal./Exp.
Neutron trap(1)	$(2.10 \pm 0.01)\times10^{13}$	$(2.15 \pm 0.08)\times10^{13}$	0.98
1-4 channel(1)	$(1.21 \pm 0.006)\times10^{13}$	$(1.25 \pm 0.05)\times10^{13}$	0.97
7-1 channel(2)	$(6.93 \pm 0.04)\times10^{12}$	$(7.0 \pm 0.3)\times10^{12}$	0.99
13-2 channel(3)	$(5.1 \pm 0.03)\times10^{12}$	$(4.9 \pm 0.2)\times10^{12}$	1.04

(1) Maximum flux point, h = 25cm
(2) Irradiation point, h = 8 cm
(3) Irradiation point, h = 4 cm

Table 3. The fitting parameters of neutron spectrum at various heights in neutron trap

Height (cm)	I_{th} ($10^{-4}n/cm^2$)	E_T (meV)	I_{epi}(10^{-5} n/cm^2)	α (10^{-2})
2	1.27 ± 0.02	26.7 ± 0.3	0.36 ± 0.07	-4.1 ± 0.4
6	2.80 ± 0.03	26.9 ± 0.3	0.80 ± 0.16	-3.8 ± 0.4
10	4.05 ± 0.05	26.9 ± 0.3	1.19 ± 0.02	-3.6 ± 0.4
14	5.04 ± 0.06	27.2 ± 0.3	1.53 ± 0.03	-3.4 ± 0.3
18	5.78 ± 0.07	27.1 ± 0.3	1.81 ± 0.03	-3.2 ± 0.3
22	6.29 ± 0.08	27.1 ± 0.3	1.93 ± 0.04	-3.3 ± 0.3
26	6.31 ± 0.09	27.1 ± 0.3	2.06 ± 0.04	-3.0 ± 0.3
30	6.21 ± 0.09	27.3 ± 0.3	1.96 ± 0.04	-2.9 ± 0.3
34	6.01 ± 0.08	27.1 ± 0.3	1.93 ± 0.04	-3.3 ± 0.3
38	5.78 ± 0.07	27.1 ± 0.3	1.81 ± 0.03	-3.2 ± 0.3
42	5.18 ± 0.06	27.1 ± 0.3	1.52 ± 0.03	-3.4 ± 0.3
46	4.46 ± 0.05	27.1 ± 0.3	1.20 ± 0.02	-3.3 ± 0.3
50	3.46 ± 0.04	27.0 ± 0.3	1.09 ± 0.02	-3.5 ± 0.3
54	2.37 ± 0.03	27.2 ± 0.3	0.70 ± 0.02	-3.7 ± 0.4
58	1.03 ± 0.02	27.3 ± 0.3	0.28 ± 0.07	-3.9 ± 0.4

Table 4. The fitting parameters of neutron spectrum at various heights in 1-4 channel

Height (cm)	I_{th} (10^{-4} n/cm^2)	E_T (meV)	I_{epi} (10^{-6}n/cm^2)	α (10^{-2})
2	0.396 ± 0.006	27.7 ± 0.3	2.33 ± 0.05	-4.3 ± 0.4
6	0.880 ± 0.010	28.0 ± 0.3	5.30 ± 0.11	-3.8 ± 0.4
10	1.231 ± 0.012	27.9 ± 0.3	7.74 ± 0.15	-3.3 ± 0.3
14	1.502 ± 0.016	28.2 ± 0.3	9.85 ± 0.20	-3.2 ± 0.3
18	1.761 ± 0.018	28.0 ± 0.3	11.9 ± 0.22	-3.1 ± 0.3
22	1.929 ± 0.020	27.8 ± 0.3	13.6 ± 0.26	-3.4 ± 0.3
26	1.910 ± 0.020	28.2 ± 0.3	15.5 ± 0.28	-3.3 ± 0.2
30	1.900 ± 0.020	28.2 ± 0.3	14.7 ± 0.27	-3.6 ± 0.3
34	1.897 ± 0.019	28.1 ± 0.3	12.8 ± 0.24	-3.8 ± 0.3
38	1.618 ± 0.017	27.9 ± 0.3	10.0 ± 0.20	-3.7 ± 0.3
46	1.074 ± 0.011	28.3 ± 0.3	6.35 ± 0.12	-3.9 ± 0.4
54	0.338 ± 0.005	28.0 ± 0.3	1.93 ± 0.04	-4.1 ± 0.4

Table 5 α-factors in irradiation channels determined from MCNP calculation and experiment

Irradiation channels	Calculated α (10^{-2})	Experimental α (10^{-2})	Cal/Exp.
Neutron trap(*)	-3.3 ± 0.3	-3.1± 0.3	1.06
1-4 channel(*)	-3.4 ± 0.4	-3.6 ± 0.4	0.94
7-1 channel(+)	-4.8 ± 0.5	-4.5 ± 0.5	1.06
13-2 channel(+)	-7.2 ± 0.7	-7.5 ± 0.8	0.96

(*) At position of maximal neutron flux
(+) At irradiation position

Table 6. Calculated and experimental cadmium ratios of gold in irradiation channels

Irradiation channels	Calculated $[R_{Cd}]_{IRDF}$	Calculated $[R_{Cd}]_{JENDL}$	Experimental $[R_{Cd}]_{EXP}$	$\frac{[R_{Cd}]_{IRDF}}{[R_{Cd}]_{EXP}}$	$\frac{[R_{Cd}]_{JENDL}}{[R_{Cd}]_{EXP}}$
Neutron trap	2.65 ± 0.08	2.75 ± 0.08	2.55 ± 0.07	1.06	1.08
1-4 channel	1.73 ± 0.05	1.77 ± 0.05	1.65 ± 0.04	1.05	1.07
7-1 channel	1.92 ± 0.06	1.98 ± 0.06	1.90 ± 0.05	1.01	1.04
13-2 channel	2.33 ± 0.07	2.38 ± 0.07	2.20 ± 0.06	1.06	1.08

- $[R_{Cd}]_{IRDF}$ and $[R_{Cd}]_{JENDL}$ are cadmium ratio of gold calculated using cross-section from IRDF82 and JENDL libraries, respectively.
- $[R_{Cd}]_{EXP}$ is experimental cadmium ratio.

Table 7. The calculated effective cross-section of $^{197}Au(n,\gamma)^{198}Au$ reaction in neutron trap and 1-4 channel using the multi-groups cross-section from IRDF82 and JENDL

Irradiation channels	$[\sigma_{eff}]_{JENDL}$	$[\sigma_{eff}]_{IRDF}$	Dif.(%)
Neutron trap	79.41	78.92	0.62
1-4 channel	64.90	64.33	0.89

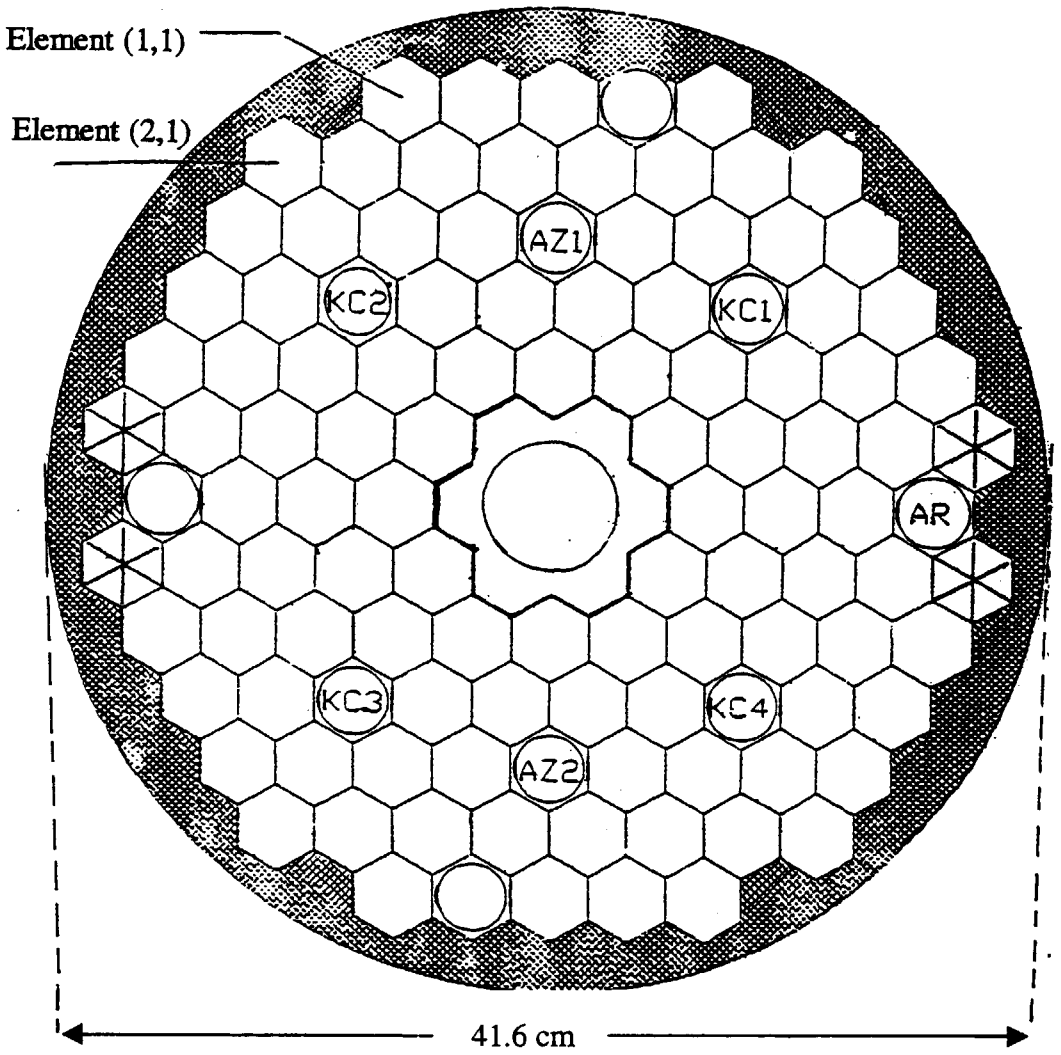

Fig. 1 Working configuration of Dalat reactor

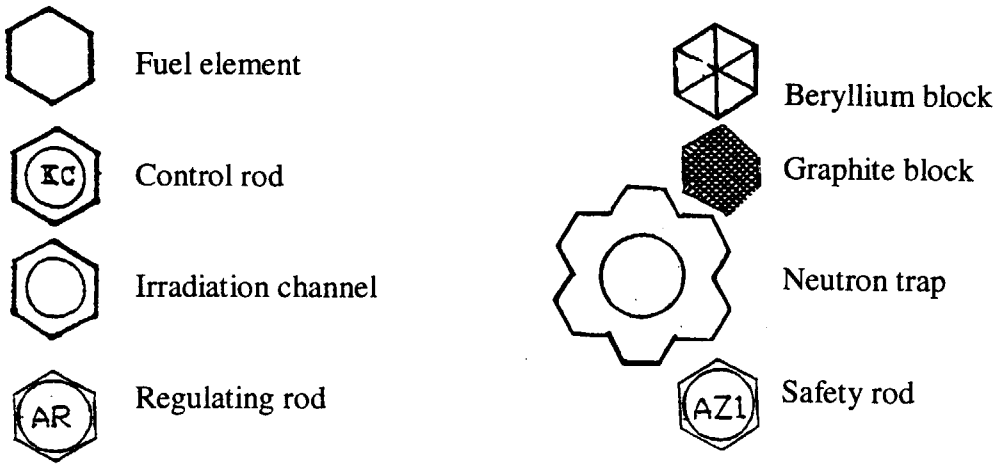

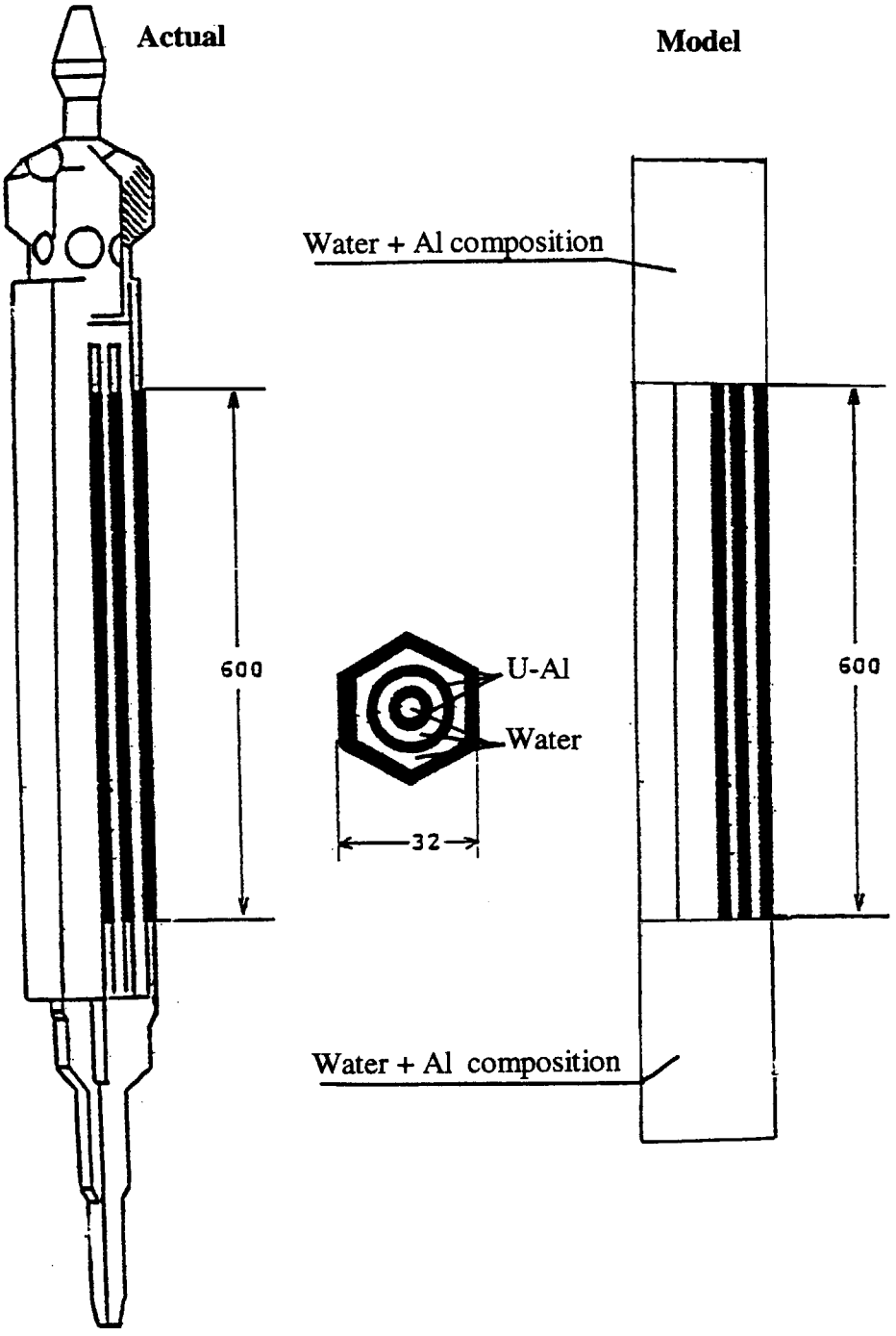

Fig. 2 The fuel element structure of Dalat reactor
(Actual structure and calculation model)

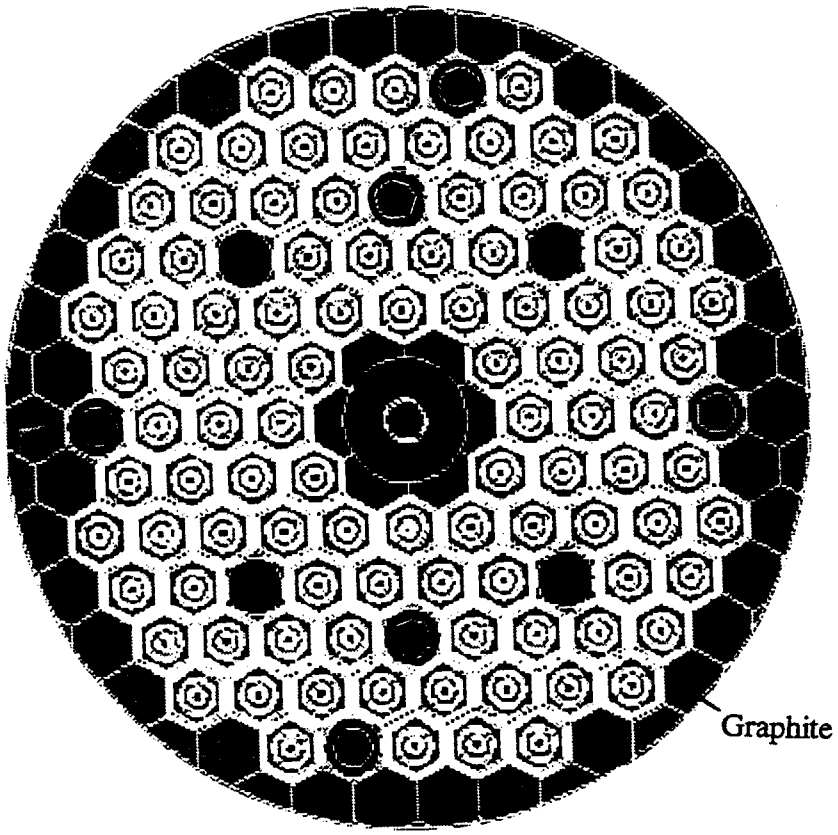

Fig. 3 Calculation configuration received from MCNP model description

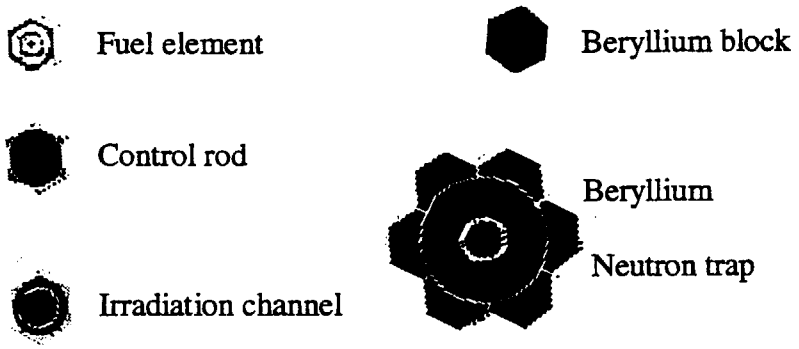

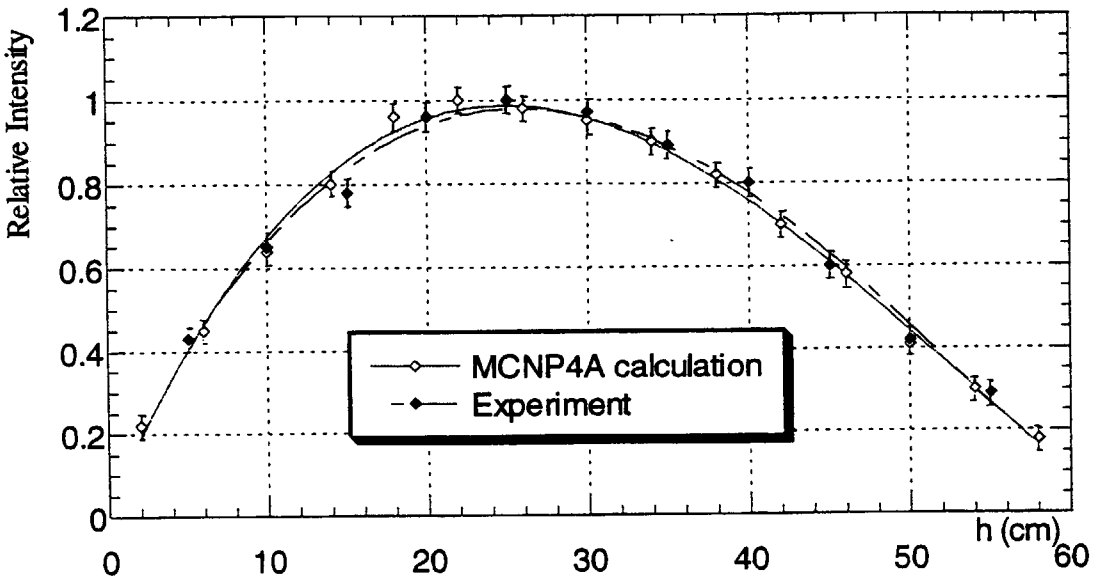

Fig.4 Distribution of neutron flux in neutron trap (MCNP calculation and experiment)

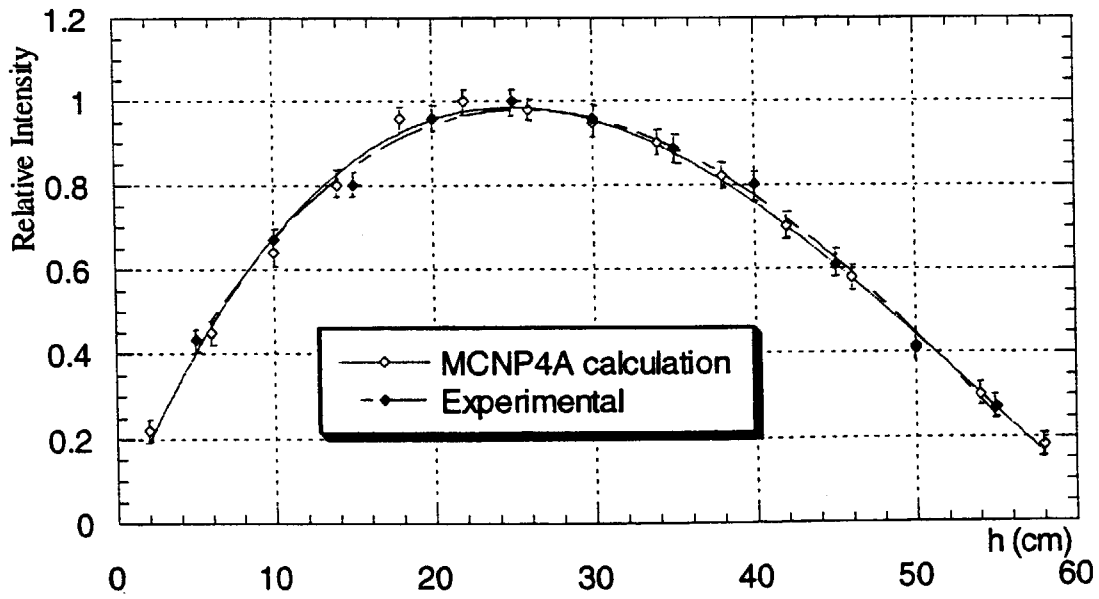

Fig.5 Distribution of neutron flux in 1-4 channel (MCNP4A calculation and experimental)

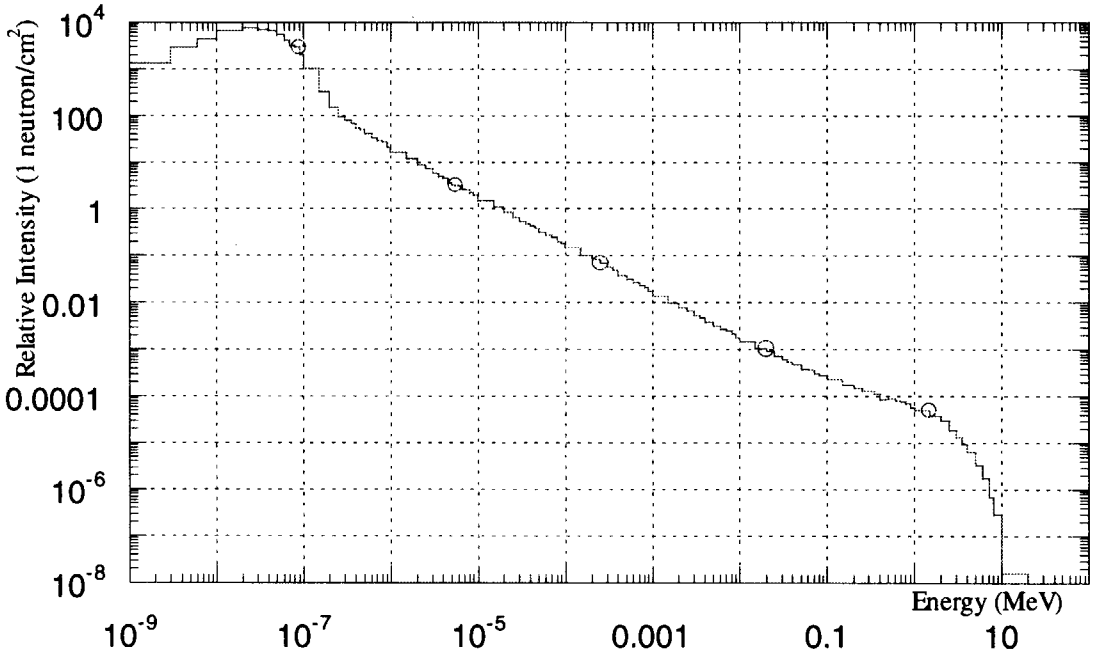

Fig.6 Calculated neutron spectrum in neutron trap (h = 22 cm)

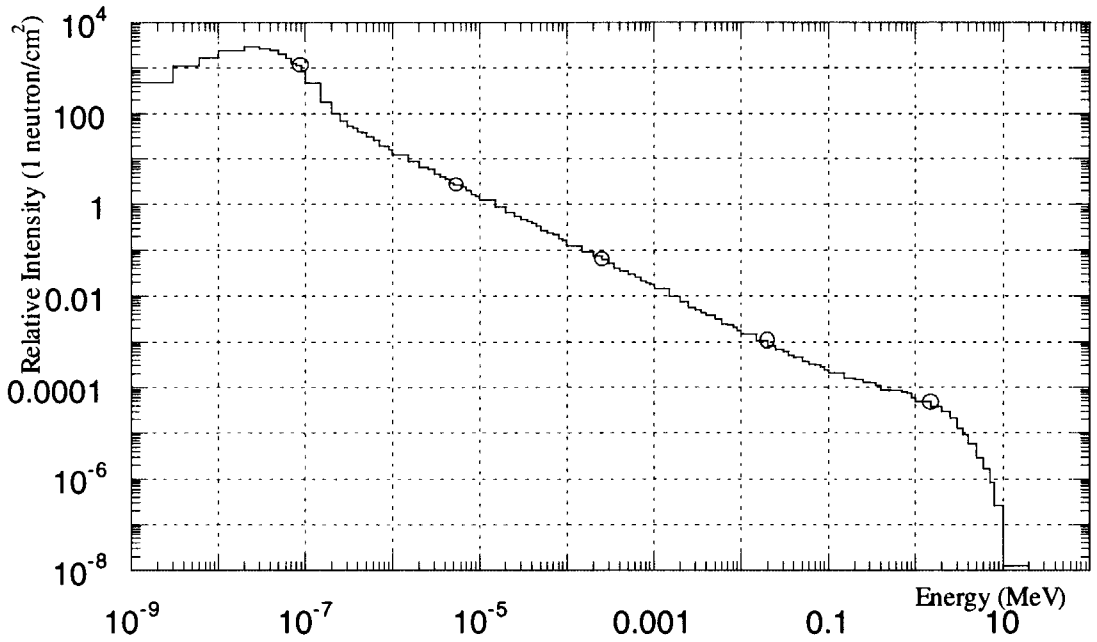

Fig.7 Calculated neutron spectrum in 1-4 channel (h = 22 cm)

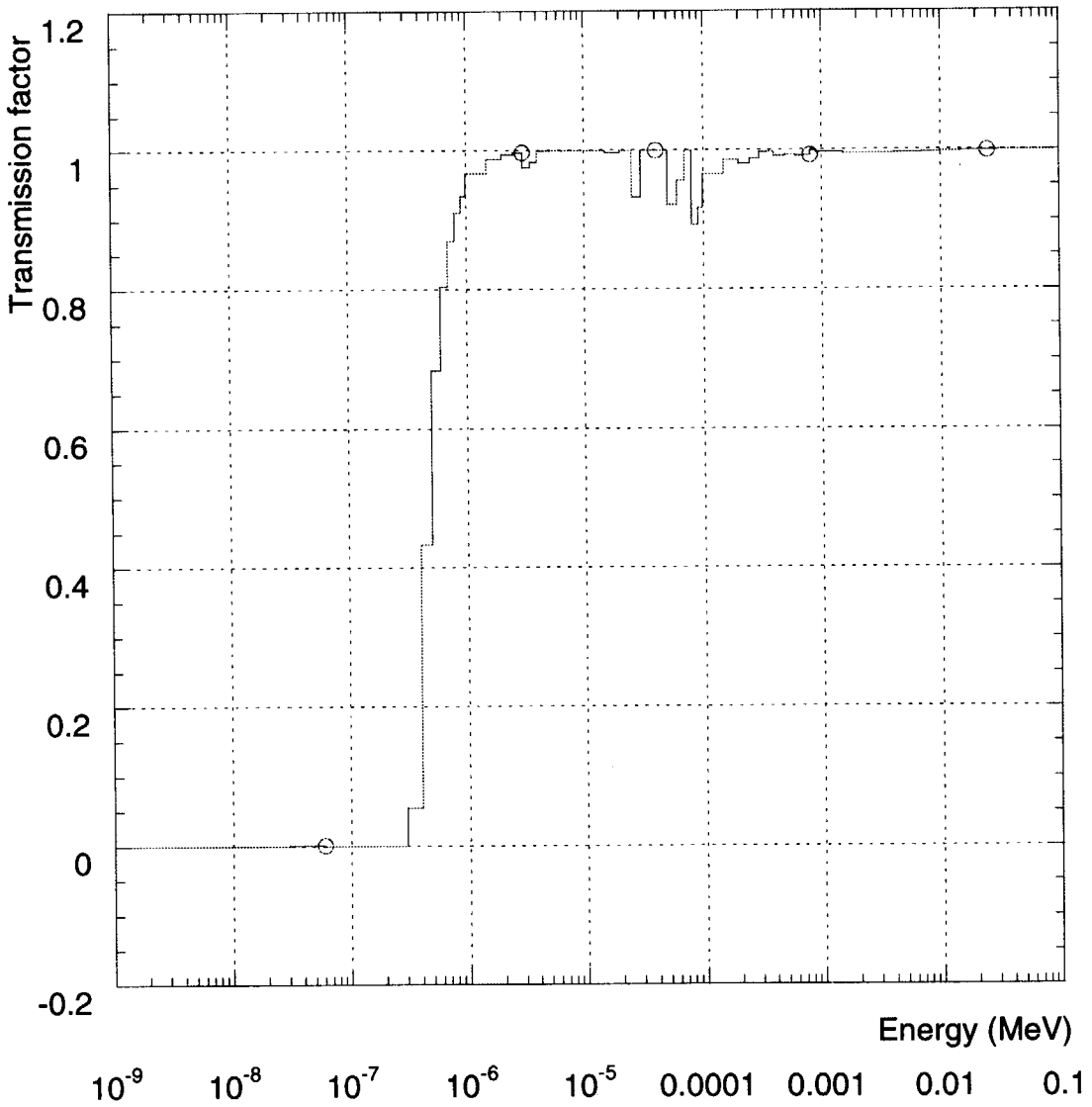

Fig.8 Neutron transmission factor of cadmium filter (thickness 0.8 mm)

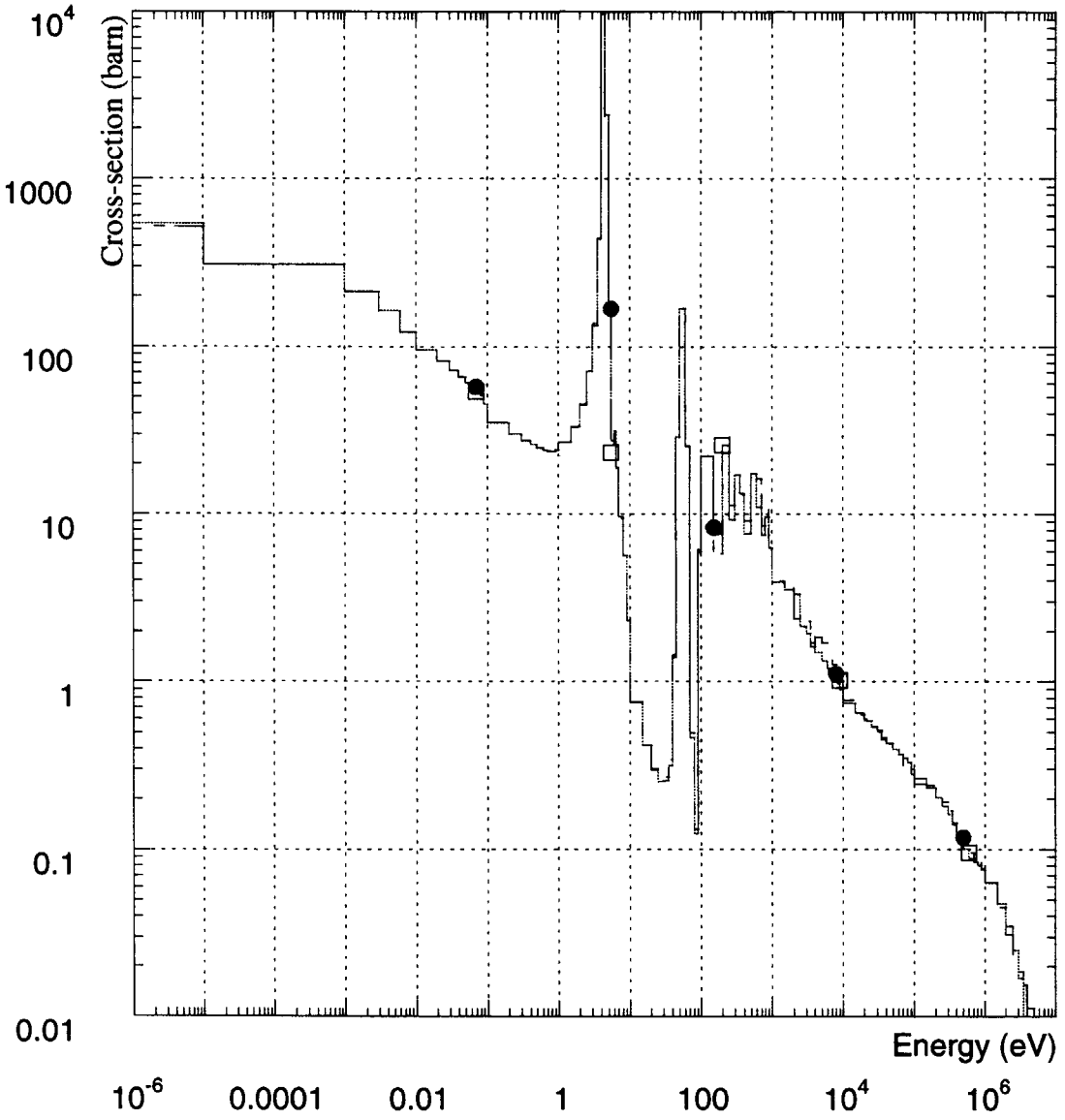

Fig.9 Cross-sections of gold from JENDL and IRDF82

(—●— JENDL, -⊡— IRDF82)

Appendix An INPUT sample for calculation of energy spectrum and neutron flux in neutron trap and 1-4 channel

```
name=inp31
1-      Prob1 – Calculation neutron flux and it's energy spectrum using MCNP4A code
2-      1     1     -1.0 –10 –101 20
3-      2     1     -1.0 –10 101 –102
4-      3     1     -1.0 –10 102 –103
5-      4     1     -1.0 –10 103 –104
6-      5     1     -1.0 –10 104 –105
7-      6     1     -1.0 –10 105 –106
8-      7     1     -1.0 –10 106 –107
9-      8     1     -1.0 –10 107 –108
10-     9     1     -1.0 –10 108 –109
11-     10    1     -1.0 –10 109 –110
12-     11    1     -1.0 –10 110 –111
13-     12    1     -1.0 –10 111 –112
14-     13    1     -1.0 –10 112 –113
15-     14    1     -1.0 –10 113 –114
16-     15    1     -1.0 –10 –30
17-     16    1     -1.0  10 –1 20 –30
18-     17    1     -1.0 –40 20 –101
19-     18    1     -1.0 –40 101 –102
20-     19    1     -1.0 –40 102 –103
21-     20    1     -1.0 –40 103 –104
22-     21    1     -1.0 -40 104 –105
23-     22    1     -1.0 –40 105 –106
24-     23    1     -1.0 –40 106 –107
25-     24    1     -1.0 –40 107 –108
26-     25    1     -1.0 –40 108 –109
27-     26    1     -1.0 –40 109 –110
28-     27    1     -1.0 –40 110 –111
29-     28    1     -1.0 –40 111 –112
30-     29    1     -1.0 –40 112 –113
31-     30    1     -1.0 –40 113 –114
32-     31    1     -1.0 –40 114 –30
33-     32    8     -1.319  –50 12 -20
34-     33    7     -0.0012 –60 20 -30
35-     34    7     -0.0012 –70 20 -30
36-     35    8     -1.319  –50 30 –13
37-     36    5     -1.68  20 –30 50 –100
38-     37    0     -50 20 –30 1 40 60 70 FILL=1
39-     38    0     100 : -12 : 13
40-     39    5     -1.68  –51 52 –53 54 55 –56 U=1 LAT=2 FILL=-7:9  -10:6  0:0
41                  1 16R
```

```
42                  1 16R
43                  1 8R 2 4 2 2R 1 2R
44                  1 6R 2 7R 1 1R
45                  1 5R 2 3R 4 2 3R 1 1R
46                  1 4R 2 1R 3 2 3R 3 2 1R 1 1R
47                  1 3R 2 10R 1 1R
48                  1 2R 5 2 3R 5 1R 2 3R 5 1 1R
49                  1 2R 4 2 2R 5 2R 2 2R 4 1 2R
50                  1 1R 5 2 3R 5 1R 2 3R 5 1 2R
51                  1 1R 2 10R 1 3R
52                  1 1R 2 1R 3 2 3R 3 2 1R 1 4R
53                  1 1R 2 3R 4 2 3R 1 5R
54                  1 1R 2 7R 1 6R
55                  1 2R 2 2R 4 2 1 8R
56                  1 16R
57                  1 16R
58          C       Universe 2: structure of control rod
59          40      3    -2.05  -80 81 u=3
60          41      1   -1.0    80: -81 u=3
61          C       Universe 3: structure of fuel rod
62          183     1   -1.0   -31 u=2
63          184     4   -2.7    31 -32 u=2
64          185     6   -1.51   32 -33 u=2
65          186     4   -2.7    33 -34 u=2
66          187     1   -1.0    34 -35 u=2
67          188     4   -2.7    35 -36 u=2
68          189     6   -1.51   36 -37 u=2
69          190     4    -2.7   37 -38 u=2
70          191     1   -1.0    38 -61 -63 65 62 64 -66 u=2
71          192     4   -2.7    (61:-62:63:-64:-65:66) 71 72 -73 74 75 -76 u=2
72          193     6   -1.51   (71:-72:73:-74:-75:76) -91 92 -93 94 95 -96 u=2
73          194     4   -2.7    91:-92:93:-94:-95:96 u=2
74          C       Universe 4: Water channel
75          205     1   -1.0   -222 u=4
76          206     4   -2.7    222 u=4
77          C       Universe 5: beryllium rod
78          210     2   -1.875  -21 22 -23 24 25 -26 u=5
79          211     5   -1.68     21:-22:23:-24:-25:26 u=5

80          1       c/z  0  -5.542725174  3.2
81          10      c/z  0  -5.542725174  1.0
82          12      pz -5.0
83          13      pz 63
84          20      pz  0.0
85          21      px  1.59
```

```
86      22      px  -1.59
87      23      p  1.0  1.732 0  3.19
88      24      p  1.0  1.732 0  -3.19
89      25      p  1.0  -1.732 0  -3.19
90      26      p  1.0  -1.732 0  3.19
91      30      pz  60.0
92      31      cz  0.17
93      32      cz  0.27
94      33      cz  0.33
95      34      cz  0.42
96      35      cz  0.76
97      36      cz  0.85
98      37      cz  0.92
99      38      cz  1.01
100     40      c/z 3.2  11.08545035  1.0
101     50      c/z 0.0  -5.542725174  20.8
102     51      pz  1.6
103     52      pz  -1.6
104     53      p   1.0  1.732  0  3.20
105     54      p   1.0  1.732  0  -3.2
106     55      p   1.0  -1.732  0 -3.2
107     56      p   1.0  -1.732  0  3.2
108     60      c/z -16.0  -5.542725174  1.0
109     61      px  1.35
110     62      px  -1.35
111     63      p   1.0  1.732  0  2.91
112     64      p   1.0  1.732  0  -2.91
113     65      p   1.0  -1.732  0  -2.91
114     66      p   1.0  -1.732  0  2.91
115     70      c/z -3.2 -22.1709 1.0
116     71      px  1.44
117     72      px  -1.44
118     73      p   1.0  1.732  0  3.01
119     74      p   1.0  1.732  0  -3.01
120     75      p   1.0  -1.732  0  -3.01
121     76      p   1.0  -1.732  0  3.01
122     80      cz  0.7
123     81      pz  16.0
124     91      px  1.51
125     92      px  -1.51
126     93      p   1.0  1.732  0  3.09
127     94      p   1.0  1.732  0  -3.09
128     95      p   1.0  -1.732  0  -3.09
129     96      p   1.0  -1.732  0  3.09
130     100     c/z  -5.542725174  30.8
```

```
131         101    pz  4.0
132         102    pz  8.0
133         103    pz  12.0
134         104    pz  16.0
135         105    pz  20.0
136         106    pz  24.0
137         107    pz  28.0
138         108    pz  32.0
139         109    pz  36.0
140         110    pz  40.0
141         111    pz  44.0
142         112    pz  48.0
143         113    pz  52.0
144         114    pz  56.0
145         222    cz  1.51

146         imp:n  1 36r 0 1 18r
147         m1     1001.37c 2  8016.37c 1
148         m2     4009.37c 1
149         m3     5010.37c –0.6870  5011.37c –0.0840  6012.37c –0.2290
150         m4     13027.37c 1
151         m5     6012.37c 1
152         m6     92235.37c –0.36 92238.37c –0.64
153         m7     1001.37c 3  8016.37c 1
154         m8     13027.37c –0.3846 1001.37c –0.06831 8016.37c –0.5469
155         mt1    lwtr.01t
156         mt2    be.01t
157         mt5    grph.01t
158         kcode  4000  1  40  3000
159         ksrc   1.5 11.08545 0.1 –1.5 11.08545 20 0.27 11.08545 11 –0.27
                   11.08545 11
160         e0     0.001e-6  0.003e-6  0.006e-6
                   0.01e-6 0.02e-6 0.03e-6 0.04e-6 0.05e-6 0.06e-6 0.07e-6 0.08e-6
                   0.09e-6 0.1e-6 0.15e-6 0.2e-6 0.25e-6 0.3e-6 0.35e-6 0.4e-6
                   0.45e-6 0.5e-6 0.6e-6 0.7e-6 0.8e-6 0.9e-6 1e-6 1.5e-6 2e-6
                    2.5e-6 3e-6 3.5e-6 4e-6 4.5e-6 5e-6 5.5e-6 6e-6 6.5e-6 7e-6
                   8e-6 9e-6 1e-5 1.5e-5 2e-5 2.5e-5 3e-5 3.5e-5 4e-5 4.5e-5 5e-5
                   6e-5 7e-5 8e-5 9e-5 1e-4 1.5e-4 2e-4 2.5e-4 3e-4 3.5e-4 4e-4
                   5e-4 6e-4 7e-4 8e-4 9e-4 1e-3 1.5e-3 2e-3 2.5e-3 3e-3 3.5e-3
                   4e-3 5e-3 6e-3 7e-3 8e-3 9e-3 1e-2 1.5e-2 2e-2 2.5e-2 3e-2 3.5e-2
                   4e-2 5e-2 6e-2 7e-2 8e-2 9e-2 1e-1 1.5e-1 2e-1 2.5e-1 3e-1 3.5e-1
                   4e-1 5e-1 6e-1 7e-1 8e-1 9e-1 1.0 1.5 2.0 2.5 3.0 3.5 4.0 5.0 6.0
                   7.0 8.0 9.0 10.0 20.0
161         f4:n   1 2 3 4 5 6 7 8 9 10 11 12 13 14 15
                   17 18 19 20 21 22 23 24 25 26 27 28 29 30 31 32 33
```

In the above geometrical description, the co-ordinate origin is chosen at the center of (5,6) element.

The cells from cell 1 to cell 35 describe ones used in the calculation of neutron spectra and flux (neutron trap, 1-4 and 13-2 channels). Cell 37 describes graphite reflector. Cell 39 describes structure of reactor core and materials. The detailed structures of materials in the reactor core, including control rods, fuel rods, beryllium, graphite blocks and water are described in cells from 40 to 221.

This is a blank page.

国際単位系 (SI) と換算表

表1　SI基本単位および補助単位

量	名称	記号
長さ	メートル	m
質量	キログラム	kg
時間	秒	s
電流	アンペア	A
熱力学温度	ケルビン	K
物質量	モル	mol
光度	カンデラ	cd
平面角	ラジアン	rad
立体角	ステラジアン	sr

表2　SIと併用される単位

名称	記号
分，時，日	min, h, d
度，分，秒	°, ′, ″
リットル	l, L
トン	t
電子ボルト	eV
原子質量単位	u

1 eV = 1.60218 × 10^{-19} J

1 u = 1.66054 × 10^{-27} kg

表3　固有の名称をもつSI組立単位

量	名称	記号	他のSI単位による表現
周波数	ヘルツ	Hz	s^{-1}
力	ニュートン	N	$m \cdot kg/s^2$
圧力，応力	パスカル	Pa	N/m^2
エネルギー，仕事，熱量	ジュール	J	N·m
工率，放射束	ワット	W	J/s
電気量，電荷	クーロン	C	A·s
電位，電圧，起電力	ボルト	V	W/A
静電容量	ファラド	F	C/V
電気抵抗	オーム	Ω	V/A
コンダクタンス	ジーメンス	S	A/V
磁束	ウェーバ	Wb	V·s
磁束密度	テスラ	T	Wb/m^2
インダクタンス	ヘンリー	H	Wb/A
セルシウス温度	セルシウス度	℃	
光束	ルーメン	lm	cd·sr
照度	ルクス	lx	lm/m^2
放射能	ベクレル	Bq	s^{-1}
吸収線量	グレイ	Gy	J/kg
線量当量	シーベルト	Sv	J/kg

表4　SIと共に暫定的に維持される単位

名称	記号
オングストローム	Å
バーン	b
バール	bar
ガル	Gal
キュリー	Ci
レントゲン	R
ラド	rad
レム	rem

1 Å = 0.1 nm = 10^{-10} m

1 b = 100 fm^2 = 10^{-28} m^2

1 bar = 0.1 MPa = 10^5 Pa

1 Gal = 1 cm/s^2 = 10^{-2} m/s^2

1 Ci = 3.7 × 10^{10} Bq

1 R = 2.58 × 10^{-4} C/kg

1 rad = 1 cGy = 10^{-2} Gy

1 rem = 1 cSv = 10^{-2} Sv

表5　SI接頭語

倍数	接頭語	記号
10^{18}	エクサ	E
10^{15}	ペタ	P
10^{12}	テラ	T
10^{9}	ギガ	G
10^{6}	メガ	M
10^{3}	キロ	k
10^{2}	ヘクト	h
10^{1}	デカ	da
10^{-1}	デシ	d
10^{-2}	センチ	c
10^{-3}	ミリ	m
10^{-6}	マイクロ	μ
10^{-9}	ナノ	n
10^{-12}	ピコ	p
10^{-15}	フェムト	f
10^{-18}	アト	a

（注）

1. 表1～5は「国際単位系」第5版，国際度量衡局 1985年刊行による。ただし，1 eVおよび1 uの値はCODATAの1986年推奨値によった。
2. 表4には海里，ノット，アール，ヘクタールも含まれているが日常の単位なのでここでは省略した。
3. barは，JISでは流体の圧力を表わす場合に限り表2のカテゴリーに分類されている。
4. EC閣僚理事会指令ではbar，barnおよび「血圧の単位」mmHgを表2のカテゴリーに入れている。

換　算　表

力	N(=10^5dyn)	kgf	lbf
	1	0.101972	0.224809
	9.80665	1	2.20462
	4.44822	0.453592	1

粘度　1 Pa·s(N·s/m^2) = 10 P(ポアズ)(g/(cm·s))

動粘度　1 m^2/s = 10^4 St(ストークス)(cm^2/s)

圧力	MPa(=10 bar)	kgf/cm^2	atm	mmHg(Torr)	lbf/in^2(psi)
	1	10.1972	9.86923	7.50062 × 10^3	145.038
	0.0980665	1	0.967841	735.559	14.2233
	0.101325	1.03323	1	760	14.6959
	1.33322 × 10^{-4}	1.35951 × 10^{-3}	1.31579 × 10^{-3}	1	1.93368 × 10^{-2}
	6.89476 × 10^{-3}	7.03070 × 10^{-2}	6.80460 × 10^{-2}	51.7149	1

エネルギー・仕事・熱量	J(=10^7erg)	kgf·m	kW·h	cal(計量法)	Btu	ft·lbf	eV
	1	0.101972	2.77778 × 10^{-7}	0.238889	9.47813 × 10^{-4}	0.737562	6.24150 × 10^{18}
	9.80665	1	2.72407 × 10^{-6}	2.34270	9.29487 × 10^{-3}	7.23301	6.12082 × 10^{19}
	3.6 × 10^6	3.67098 × 10^5	1	8.59999 × 10^5	3412.13	2.65522 × 10^6	2.24694 × 10^{25}
	4.18605	0.426858	1.16279 × 10^{-6}	1	3.96759 × 10^{-3}	3.08747	2.61272 × 10^{19}
	1055.06	107.586	2.93072 × 10^{-4}	252.042	1	778.172	6.58515 × 10^{21}
	1.35582	0.138255	3.76616 × 10^{-7}	0.323890	1.28506 × 10^{-3}	1	8.46233 × 10^{18}
	1.60218 × 10^{-19}	1.63377 × 10^{-20}	4.45050 × 10^{-26}	3.82743 × 10^{-20}	1.51857 × 10^{-22}	1.18171 × 10^{-19}	1

1 cal = 4.18605 J（計量法）
= 4.184 J （熱化学）
= 4.1855 J （15 °C）
= 4.1868 J（国際蒸気表）

仕事率　1 PS（仏馬力）
= 75 kgf·m/s
= 735.499 W

放射能	Bq	Ci
	1	2.70270 × 10^{-11}
	3.7 × 10^{10}	1

吸収線量	Gy	rad
	1	100
	0.01	1

照射線量	C/kg	R
	1	3876
	2.58 × 10^{-4}	1

線量当量	Sv	rem
	1	100
	0.01	1

（86年12月26日現在）